ACS Catalysis

Research Article

pubs.acs.org/acscatalysis

Aqueous-Phase Methane Oxidation over Fe-MFI Zeolites; Promotion through Isomorphous Framework Substitution

Ceri Hammond,*[,†,∥] Nikolaos Dimitratos,[†,⊥] Jose Antonio Lopez-Sanchez,[†,#] Robert L. Jenkins,[†] Gareth Whiting,[†] Simon A. Kondrat,[†] Mohd Hasbi ab Rahim,[†] Michael M. Forde,[†] Adam Thetford,[†] Henk Hagen,[‡] Eric E. Stangland,[§] Jacob M. Moulijn,[†] Stuart H. Taylor,[†] David J. Willock,[†] and Graham J. Hutchings*[,†]

[†]Cardiff Catalysis Institute, School of Chemistry, Cardiff University, Main Building, Park Place, Cardiff CF10 3AT, U.K.

[‡]Dow Benelux B. V., Herbert H. Dowweg 5, 4542 NM HOEK, Postbus 48, 4530 AA Terneuzen, The Netherlands

[§]National Corporate R&D, The Dow Chemical Company, Midland, Michigan 48674, United States

Supporting Information

ABSTRACT: Fe- and Cu-containing zeolites have recently been shown to be efficient catalysts for the one-step selective transformation of methane into methanol in an aqueous medium at only 50 °C, using H_2O_2 as green oxidant. Previously, we have observed that Fe species alone are capable of catalyzing this highly selective transformation. However, further catalytic testing and spectroscopic investigations demonstrate that although these extra-framework Fe species are the active component of the catalyst, significant promotion is observed upon the incorporation of other trivalent cations, e.g., Al^{3+} or Ga^{3+}, into the MFI-framework. While these additional framework species do not constitute active catalytic centers, promotion is observed upon their incorporation as they (1) facilitate the extraction of Fe from the zeolite framework and hence increase the formation of the active Fe species and (2) provide an associated negatively charged framework, which is capable of stabilizing and maintaining the dispersion of the cationic extra-framework Fe species responsible for catalytic activity. By understanding these phenomena and subsequently controlling the overall composition of the catalyst (Fe *and* Al), we have subsequently been able to prepare a catalyst of equal intrinsic activity (i.e., TOF) but five-times higher productivity (i.e., space-time-yield) compared with the best catalysts reported for this reaction to date.

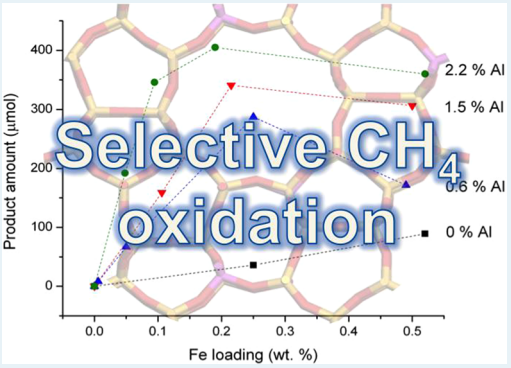

KEYWORDS: *methane oxidation, zeolite catalysis, selective oxidation, natural gas upgrading, sustainable chemistry*

INTRODUCTION

Natural gas is a highly abundant source of hydrocarbons that is primarily composed of methane (ca. 85 vol. %), and represents one of the major building blocks of the present day chemical industry.[1−3] Nevertheless, its conversion to various chemicals and fuels currently requires the intermediate manufacture of synthesis gas and subsequent conversion to higher hydrocarbons or commodity chemicals through Fischer−Tropsch-type chemistry.[4] During various stages of these processes, extremely high temperatures and pressures are required, thus resulting in high operational costs and significant capital investment.

As such, the development of alternative and less economically intensive routes for the selective transformation of natural gas, or methane in particular, to various value-added products is of particular interest. Of greatest promise is the transformation of methane to more energy-dense liquid derivatives, such as methanol, formic acid, or midrange hydrocarbons. Along with being useful as chemical building blocks, e.g., methanol-to-olefin technology,[5] these liquid derivatives are significantly easier and cheaper to transport around the globe; like many fossil reserves, a large fraction of the natural gas reserves is inconveniently located in various inaccessible parts of the globe. In contrast to crude oil, the transportation of this volatile and flammable gas to existing technological sites presents considerable safety and economic issues. The conversion of methane to more energy dense liquid derivatives, particularly at the point of origin, could lead to significant breakthroughs in the utilization of natural gas as a primary feedstock.

The primary obstacle and more challenging aspect of this reaction stems from the fact that methane is the least reactive of all hydrocarbons, with very high C−H bond strengths of 438.8 kJ mol^{-1}. Consequently, conditions that are sufficient to activate methane also have the undesired effect of activating the partial oxidation products toward deeper oxygenated products (CO_x), since bond strengths in these oxygenated species are

Received: April 16, 2013
Revised: June 28, 2013
Published: July 2, 2013

   dx.doi.org/10.1021/cs400288b | ACS Catal. 2013, 3, 1835−1844

typically much lower (ΔH_{C-H} = 373.5 kJ mol^{-1} for methanol). Thus, at high temperatures the formation of deeper oxygenated products such as CO and CO_2 is generally unavoidable, which limits the overall reaction selectivity. In view of this, it is apparent that the selective oxidation of methane can only be achieved by developing new catalytic systems that are able to oxidize methane at mild temperatures (≤200 °C), as this may provide some inherent selectivity to the partial oxidation products by operating under kinetic rather than thermodymanic control.

While a number of low temperature approaches have been proposed in recent times, each approach is typically limited by low catalytic rates, i.e., low turnover frequencies/space-time-yields or environmental issues concerning the solvent system or chosen oxidant.[1] For example, while the electrophillic activation of methane by bipyramidal platinum complexes yields methyl bisulphate at high selectivity (81% at >90% conversion), this and related systems are limited by the highly corrosive solvent system (oleum), low intrinsic activity (TOF < 10 h^{-1}), and the lack of a fully closed catalytic cycle.[6,7] An alternative approach has focused upon on the use of Fe(Cu)-containing zeolites for the selective oxidation of methane with $N_2O(O_2)$.[8−13] While these materials do exhibit a remarkable ability to activate methane, the product in both cases is a strongly chemisorbed methoxy species that cannot be readily desorbed or isolated without destruction of the catalytic active sites, thus resulting in a noncatalytic process. Alternative approaches using both encapsulated[14] or supported[15,16] Fe-phthalocyanine complexes have also been proposed, but these systems are limited by very low intrinsic activities, maximum methanol selectivities of 50%, and catalyst stability issues.[17]

We have demonstrated not only that Fe-containing MFI-type zeolites are capable of oxidizing methane at high catalytic rates (≤14,500 h^{-1}) and partial oxygenate selectivity, i.e., selectivity to oxidation products not including CO and CO_2 (≥90%) but also that this favorable transformation can be carried out in an environmentally benign process at only 50 °C, in the aqueous phase, and with hydrogen peroxide as the chosen oxidant.[18] Moreover, although the Fe-only system was primarily selective to formic acid, we have demonstrated that the addition of Cu^{2+} to these highly reactive Fe-containing zeolites eliminates the methanol overoxidation process, thereby allowing methanol to be obtained at over 90% selectivity at methane conversions of up to 10%.[18,19]

Recently, we demonstrated that the catalytic activity of these materials corresponds to the formation of extra-framework Fe^{3+} species that reside within the zeolite micropores.[20] While bearing some resemblance to the solid-state chemistry exhibited by these materials during activation for N_2O-based oxidations, key evidence has indicated that the active species formed in this system for selective and catalytic methane oxidation with H_2O_2 are fundamentally different from those found for these other stoichiometric oxidation systems, given the different preactivation procedures employed.[20] However, a major question remains. While Fe *alone* in Fe-silicalite-1 is capable of catalyzing the reaction, significantly higher turnover frequencies have been observed for an Fe- and Al-containing systems (such as commercial zeolite ZSM-5), despite the catalytic inactivity of Al^{3+} and its related properties for this reaction.[18] In this publication we now focus on this key aspect in order to develop a more detailed understanding of this unique methane oxidation catalyst and subsequently produce significantly more active catalysts for this challenging reaction.

RESULTS AND DISCUSSION

Material Synthesis. To determine the precise role(s) of Al^{3+}, analogous samples of silicalite-1, ZSM-5, Fe-silicalite-1, and Fe-ZSM-5 were first prepared by hydrothermal synthesis. In particular, this was necessary in order to avoid issues associated with comparing samples obtained from different sources (commercial material vs laboratory prepared material) and that contained different Fe loadings. To achieve this comparison, Al-only (ZSM-5), Fe-only (Fe-silicalite-1), Fe- and Al-containing (Fe-ZSM-5), and metal-free (silicalite-1) analogues were prepared by an identical, benchmarked[20] hydrothermal synthesis procedure (Table 1) and later screened for activity (Table 2). We note here that the pretreatment temperature employed during activation of the catalyst is provided as a subscript following the description of the catalyst and that the SiO_2/Al_2O_3 ratio, where applicable, is provided in parentheses. Additionally, the Fe loading of the catalyst, where applicable, is provided prior to the catalyst description, e.g., Fe-containing ZSM-5, containing 0.5 wt % Fe and a SiO_2/Al_2O_3 mole ratio of 84 and pretreated at 550 °C, is denoted 0.5Fe-ZSM-5 $(84)_{550}$. As demonstrated by XRD analysis (Supplementary Figure S1), each of the synthesized samples possesses the crystalline MFI structure. Coupled with the similar surface areas (±330 m^2 g^{-1}) and microprorous volumes (±0.13 cm^{-3} g^{-1}), it can be concluded that each synthesized solid possesses comparable physical properties. In view of this, each sample was subsequently evaluated for catalytic activity following activation at 550 °C.

Table 1. Physical and Chemical Properties of a Series of Al- and Fe-Containing MFI-Type Zeolites, Prepared by Hydrothermal Synthesis

		molar ratio			
catalyst	Fe content (wt %)[a]	SiO_2/Fe_2O_3	SiO_2/Al_2O_3	S_{BET} (m^2 g^{-1})	V_{MICRO} (cm^3 g^{-1})
silicalite-1_{550}	<0.001			330	0.13
ZSM-5 $(86)_{550}$	0.003		86	340	0.14
Fe-silicalite-1_{550}	0.52	250		330	0.13
Fe-ZSM-5 $(84)_{550}$	0.49	254	84	310	0.14

[a]Determined by ICP-OES. Values are accurate to ±10%.

In line with our previous studies, the synthesis of metal-free silicalite-1_{550} and Al-only ZSM-5 $(86)_{550}$ does not lead to materials with any significant activity for this reaction.[18−20] This is in agreement with our previous observations that catalytic activity for methane oxidation with H_2O_2 can only be achieved when sufficient quantities of Fe^{3+} are present within the catalyst and that the presence of Brønsted and Lewis acid sites (from framework Al^{3+}) and/or a microporous framework alone are insufficient for catalysis to be observed. In fact, we have previously attributed the very minor catalytic activity of our synthesized ZSM-5 materials to be related to their low but non-negligible Fe^{3+} content (Table 1).[20]

The requirement for Fe^{3+} is well emphasized by comparing entries 1 and 3 of Table 2, where it can be observed that the incorporation of a low amount of Fe^{3+} (0.5 wt %) into the inactive silicalite-1 material leads to large increases in catalytic activity. As expected in the absence of a Cu^{2+} additive, which we have shown to be critical for maintaining MeOH selectivity,[18−20] the major product formed with 0.5Fe-silicalite-1 is HCOOH (at 62% selectivity), though the selectivity to partial

dx.doi.org/10.1021/cs400288b | ACS Catal. 2013, 3, 1835−1844

Table 2. Catalytic Activity of Analogous Samples of a Series of Al- and Fe-Containing MFI-Type Zeolites, Prepared by Hydrothermal Synthesis[a]

	product amount (μmol)					
catalyst	MeOH	HCOOH	MeOOH	CO_2 (g)	sum of products (μmol)	oxy sel (%)
silicalite-1_{550}	0.0	0.0	0.0	0.0	0	
ZSM-5 $(86)_{550}$	1.5	0.8	2.3	1.6	6.2	74
Fe-silicalite-1_{550}	17.6	56.1	11.0	6.4	91.1	93
Fe-ZSM-5 $(84)_{550}$	20.1	158.5	3.0	15.8	197.4	92

[a]Reaction conditions: cat., various (27 mg); $P_{(CH_4)}$, 30.5 bar; $[H_2O_2]$, 0.5 M; temp, 50 °C; time, 30 min; stirring speed, 1500 rpm.; Note: each catalyst was calcined at 550 °C for 3 h in air prior to use.

oxygenates (MeOOH, MeOH, and HCOOH) remains high (93%) and the selectivity to CO_2 (7%) remains very low.

Nevertheless, despite the minimal catalytic activity of Al-only ZSM-5 (entry 2, Table 2), 0.5Fe-ZSM-5 (84), again comprising only 0.5 wt % Fe, is over 2 times more active than the analogous sample of 0.5Fe-silicalite-1, following the addition of only 0.6 wt % Al (Table 2, compare entry 4 vs entry 3). Additionally, although the catalyst is over twice as active, no significant loss of partial oxygenate selectivity was observed (92%), though HCOOH selectivity was marginally higher (80%), likely as a consequence of the increased conversion. Given that these samples were prepared by the same method and contain similar physical and chemical properties (Fe content, surface areas, and pore volumes), it is highly unlikely that the reactivity differences observed can be related to changes in the physical properties of the zeolite or potential secondary factors such as diffusion. Indeed, it can be assumed that the only difference in these samples is the Al^{3+} content and hence the simultaneous presence of Fe^{3+} and Brønsted/Lewis acid sites. This conclusively demonstrates that the presence of Al^{3+} is highly beneficial to the activity of the catalyst. While it cannot be forgotten that the addition of Al^{3+} does increase the hydrophilicity of the MFI framework, the very dilute levels of Al^{3+} in 0.5Fe-ZSM-5 $(84)_{550}$ (SiO_2/Al_2O_3 = 84) does not majorly change the hydrophobic nature of the sample, and since the diffusion of both a hydrophobic (methane) and hydrophilic (H_2O_2) reactant is required for reaction, changes in the hydrophil-/phob-icity of the samples is unlikely to be responsible for the observed difference in catalytic activity. We stress here that, in agreement to our previous publications,[18−20] each catalyst was found to be heterogeneous, i.e., leaching of an active homogeneous catalyst into solution did not occur (Supplementary Figure S2).

This raises the important question of the precise role(s) of Al^{3+}. Indeed, even for the more thoroughly established N_2O-based oxidations, the role(s) of Al^{3+} in the same or similar materials is still the subject of much debate. For instance, Hensen et al. have reported that only MFI materials containing both Fe and Al exhibit catalytic activity for N_2O-based oxidations, as the active site in these cases is an extra-framework mixed oxide (Fe-O-Al).[21] A number of other reports also conclude that Al^{3+} itself or the Brønsted acid sites associated with framework Al^{3+} also constitute active catalytic centers for such reactions.[22] It has also been reported that Al^{3+} facilitates the autoreduction of Fe^{3+} to Fe^{2+}, which is the active state of Fe for both benzene hydroxylation and N_2O decomposition. Furthermore, the ability of Al^{3+} to aid the extraction of Fe^{3+} from the framework of the zeolite (and thus form active extra-framework species) is also widely reported.[23] Finally, it is also known that the associated cation-exchange site of the AlO_4 tetrahedron is able to stabilize cationic extra-framework complexes.[24,25] Nevertheless, it should not be overlooked that the activation procedures employed for this reaction are fundamentally different to those utilized for N_2O-based oxidations and that different Fe species apparently catalyze these different reactions.

Extraction of Framework Fe^{3+}. We have previously demonstrated that although a homogeneous distribution of framework Fe^{3+} is found within as synthesized zeolite, significant changes to the speciation of Fe^{3+} are observed following the two heat pretreatment procedures required to (1) remove the residual organic template and (2) further activate the material prior to catalysis (Scheme 1).[20] Specifically, we

Scheme 1. Activation Procedures Employed for 0.5Fe-Silicalite-1 and 0.5Fe-ZSM-5 (84)[a]

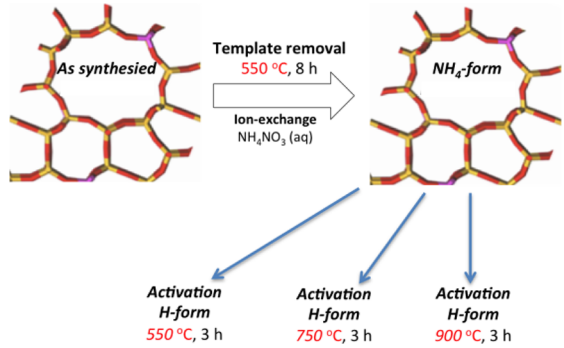

[a]Removal of the template at 550 °C and ion exchange with NH_4NO_3 leads to an NH_4-form zeolite. Further activation (≥550 °C) yields the H-form of the zeolite. This scheme was originally published in ref 20.

observed that during removal of the organic template (pretreatment 1) and further activation (pretreatment 2), Fe^{3+} migrates from coordinatively saturated framework sites, to form extra-framework Fe^{3+} cations that take up position within the zeolite channels. Indeed, this migration to the extra-framework was found to be a prerequisite for attaining high levels of activity, and a positive correlation (R^2 = 0.92) between the fraction of these species and catalytic activity was observed.[20] Considering this, it seemed important to us to establish whether the migration of Fe^{3+} to the extra-framework is greater when Al^{3+} is also present in the structure. In fact, it has previously been reported that along with Fe^{3+} being less stable than Al^{3+} in the ZSM-5 framework, the stability of Fe^{3+} within the MFI framework is significantly lower in ZSM-5 than in silicalite-1.[21]

The ligand to metal charge transfer (LMCT) bands ($Fe^{3+}\leftarrow$ O) within the UV−vis spectra of Fe-containing zeolites is an ideal method for studying the extraction of Fe^{3+} from the

dx.doi.org/10.1021/cs400288b | ACS Catal. 2013, 3, 1835−1844

framework of the zeolite, due to the distinct absorbances found for Fe species in different geometrical positions and coordination environments within the zeolite.[26−31] There are of course some inherent limitations in regards to utilizing UV−vis as a fully quantitative tool. For example, deviations in the precise molar extinction coefficients (ε) of various absorbing species and the presence of (multiple) broad, overlapping bands make full quantification an extreme challenge. Nevertheless, for Fe-containing zeolites, it has been shown that the ε values are equal to the same order of magnitude[32] and that the multiple bands can adequately be fitted by using single bands corresponding to (1) framework Fe species (200−250 nm, λ_1), (2) isolated and oligomeric extra-framework Fe cations within the zeolite channels (250−350 nm, λ_2), (3) larger Fe clusters (350−450 nm, λ_3,) and finally (4) bulk Fe oxides on the surface of the zeolite (>450 nm, λ_4). Moreover, any deviations of these factors will also be systematic over the entire series of pretreated catalysts and will still provide empirical and semiquantitative insights in regards to the precise changes in speciation of Fe^{3+} in these materials as a function of pretreatment and/or Al^{3+} incorporation.

Given the increased levels of absorbance at wavelengths at or above 250 nm, which correspond to extra-framework Fe^{3+} species, it is clear that following template removal and identical activation procedures (550 °C, 3 h in air), more extensive Fe^{3+} migration has indeed taken place in 0.5Fe-ZSM-5 $(84)_{550}$ versus 0.5Fe-silicalite-1_{550} (Figure 1). Given that our previous studies

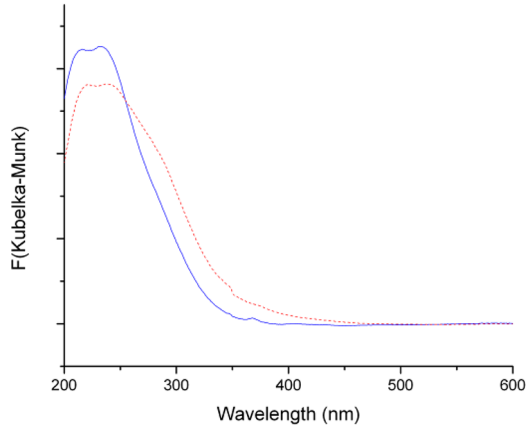

Figure 1. Diffuse reflectance UV−vis spectra for 0.5Fe-silicalite-1_{550} (blue/solid) and 0.5Fe-ZSM-5 $(84)_{550}$ (red/dashed) both containing ±0.5 wt % Fe^{3+} and calcined at 550 °C in air.

correlated catalytic activity to extra-framework Fe species within the zeolite micropores,[20] it is logical that the increased dislodgement of framework Fe^{3+} to the extra-framework observed for 0.5Fe-ZSM-5_{550} at identical pretreatment temperatures would result in an increase in catalytic activity.

The relationship between extra-framework Fe species within the micropores and catalytic activity, especially in regards to the disparate activities of 0.5Fe-ZSM-5 (90) and 0.5Fe-silicalite-1, is even more clearly displayed through full deconvolution of the observed UV−vis spectra into the four relevant sub-bands (Table 3).

Although the aforementioned issues do not allow us to calculate an exact percentage of each type of Fe species, calculating the relative contributions of each area of the UV−vis absorption spectra demonstrates that while significant Fe^{3+} migration is observed for the activated form of 0.5Fe-

Table 3. Deconvolution Data for 0.5Fe-Silicalite-1_{550} and 0.5Fe-ZSM-5 $(84)_{550}$, Both Containing ±0.5 wt % Fe^{3+}, after Template Removal and Heat Pre-treatment at 550 °C

	relative contribution of each λ range (nm)			
catalyst	λ_1	λ_2	λ_3	λ_4
0.5Fe-silicalite-1_{550}	0.627	0.337	0.025	0.011
0.5Fe-ZSM-5 $(84)_{550}$	0.422	0.542	0.027	0.009

silicalite-1_{550}, it is evident that, following identical heat pretreatment procedures, significantly more Fe^{3+} has migrated from the tetrahedral framework sites in 0.5Fe-ZSM-5 $(84)_{550}$. In fact, following template removal and activation at 550 °C, the majority of Fe^{3+} can be assigned to extra-framework species in 0.5Fe-ZSM-5 $(84)_{550}$, clearly displaying the remarkably low stability of framework Fe^{3+} in this sample. This also demonstrates the lower stability of framework Fe^{3+} in ZSM-5 compared with that in silicalite-1, an observation that is supported by the available literature.[21]

Most notably, a significantly higher fraction of extra-framework Fe cations within the micropores is present in 0.5Fe-ZSM-5 $(84)_{550}$ than in 0.5Fe-silicalite-1_{550}. This is highly significant, as we have previously demonstrated through computational[18] and spectroscopic[20] studies that these Fe^{3+} species are most likely the species that are responsible for the catalytic activity displayed by this catalyst the for selective oxidation of methane. In fact, if one were to assume that *all* of these Fe species in these samples were active and that no other Fe species impact catalytic activity whatsoever, we would expect 0.5Fe-ZSM-5 $(84)_{550}$ to be around 1.6 times more active than 0.5Fe-silicalite-1_{550} under these conditions, which is in good, but not perfect, agreement to the observed activities, 0.5Fe-ZSM-5 $(90)_{550}$ being 2.1 times more active than 0.5Fe-silicalite-1_{550} (Table 2). We stress here that through UV−vis spectroscopy alone it is not possible to be more specific regarding the nature and composition of these extra-framework species, as there are a large number of potential species that could contribute to this broad absorbance feature, i.e., isolated extra-framework Fe^{3+} species, dimers, trimers, and small oligomers are all expected to absorb within this region. However, while not the purpose of this publication, our previous EXAFS studies and DFT calculations have suggest that the active extra-framework clusters contain between one and three Fe atoms, with the best match for experiment and theory being obtained for $Fe_2(\mu_2\text{-}OH)_2(OH)_2(H_2O)_2]^{2+}$, a binuclear active site that comprises an overall +2 charge.[18]

It seems reasonable, therefore, that since greater Fe^{3+} migration is observed in 0.5Fe-ZSM-5 $(84)_{550}$ than in 0.5Fe-silicalite-1_{550} following identical activation procedures, the Al-containing analogue would display higher levels of activity. In such a case, Al^{3+} would not so much act as a catalytic promoter but behave as a structural promoter for increasing the probability of forming the active species. In such a case, it should be possible to form an equally active sample of 0.5Fe-silicalite-1_{550} just by increasing the pretreatment (activation) temperature, in order to obtain a similar distribution of Fe^{3+} species. To verify whether the increased activity observed for 0.5Fe-ZSM5 $(84)_{550}$ over 0.5Fe-silicalite-1_{550} was simply due to an insufficient pretreatment of Fe-silicalite-1, i.e., whether Al^{3+} did indeed promote the catalyst, or if the pretreatment of Fe-silicalite-1 was simply not optimized to achieve the same level of extra-framework Fe^{3+} and hence activity, both NH_4-form samples of 0.5Fe-ZSM-5 (84) and 0.5Fe-silicalite-1 were

pretreated at different temperatures, in order to determine the maximum activity possible for each sample (Figure 2).

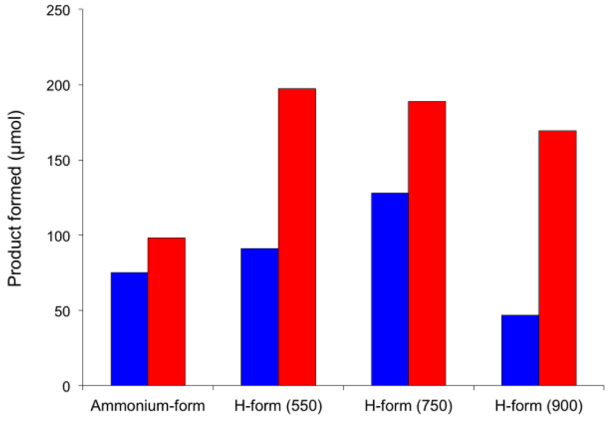

Figure 2. Catalytic activity of 0.5Fe-silicalite-1 (blue bars/left) and 0.5Fe-ZSM-5 (84) (red bars/right), following high temperature pretreatment. The temperature of pretreatment is denoted in parentheses. Reaction conditions: cat., various (27 mg); $P_{(CH_4)}$, 30.5 bar; [H_2O_2], 0.5 M; temp, 50 °C; time, 30 min; stirring speed, 1500 rpm; catalyst pretreatment, various °C, 3 h, air.

As we previously demonstrated for 0.5Fe-silicalite-1, both ammonium-form samples of 0.5Fe-silicalite-1_{NH_4} and 0.5Fe-ZSM-5_{NH_4} show considerable levels of activity due to the migration of Fe^{3+} from the framework sites that occurs during removal of the organic template (Scheme 1). Nevertheless, considerable increases in catalytic activity of both materials can be achieved following a second high-temperature pretreatment. However, while it is clear that an activation temperature of 550 °C is optimal for 0.5Fe-ZSM-5 $(84)_{550}$, 0.5Fe-silicalite-1 does not reach its maximum catalytic activity until a pretreatment temperature of 750 °C is utilized. At significantly higher pretreatment temperatures (900 °C), both 0.5Fe-silicalite-1 and 0.5Fe-ZSM-5 (84) decrease in activity, though the observed decrease is significantly greater for Fe-silicalite-1.

Nevertheless, despite the fact that the optimal pretreatment of Fe-silicalite-1 is ca. 200 °C higher than for Fe-ZSM-5, 0.5Fe-silicalite-1 is *always* less active than 0.5Fe-ZSM-5 (84), even following optimization of both catalyst pretreatment procedures. This is in direct contrast to previous studies focusing on Fe-containing zeolites for N_2O decomposition, which demonstrated that the catalytic activity of Fe-silicalite-1 and Fe-ZSM-5 are identical for NO_x decomposition following optimization of the pretreatments.[28] This clearly indicates that in the case of Fe-containing zeolites for aqueous-phase methane oxidation, there is an additional promotional role of Al^{3+} in the catalyst beyond simply facilitating the extraction of Fe^{3+} species to the extra-framework.

This is further emphasized from the deconvolution analysis of 0.5Fe-ZSM-5 (84) and 0.5Fe-silicalite-1, following heat pretreatment (Supplementary Table S1 and Figure S3 and ref 20, respectively). Previously, we have demonstrated that the activity of 0.5Fe-silicalite-1 correlates well with the amount of extra-framework Fe within the zeolite micropores, i.e., λ_2. A similar interpretation of the UV−vis data of 0.5Fe-ZSM-5 (84) also produces a positive correlation between the percentage of these species and catalytic activity (Figure 3). Nevertheless, it is clear that per "active" Fe species, 0.5Fe-ZSM-5 (84) displays over 20% higher activity compared with that of 0.5Fe-silicalite-1.

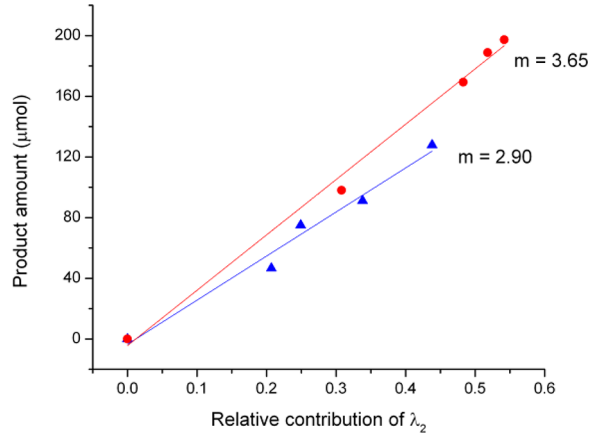

Figure 3. Relationship between the fraction of extra-framework Fe species within the zeolite micropores (the proposed active species) and catalytic activity for 0.5Fe-silicalite-1 (▲) and 0.5Fe-ZSM-5 (84) (●) following various pretreatment procedures. The data for 0.5Fe-silicalite-1 were previously published in ref 20.

Role of Cation-Exchange Sites. An additional promotional role of Al^{3+} was inferred by visual inspection and kinetic evaluation of the samples calcined at 900 °C; while the 0.5Fe-ZSM-5 $(84)_{900}$ sample was still white in color and comparable in activity to those samples pretreated at 550 °C, the 0.5Fe-silicalite-1_{900} sample was a dark orange/brown color and significantly less active than the samples calcined at 550 and 750 °C. This implies that excessive clustering to catalytically inactive bulk Fe oxides is more evident in the Fe-only sample, despite the fact that Fe^{3+} is initially more easily extracted from the Fe- and Al-containing system. We have previously identified bulk Fe oxides to be not only incapable of methane activation but also responsible for the formation of carbon oxide species and increased nonselective H_2O_2 decomposition.[20] Thus, the decrease in the percentage of "active" Fe species, coupled with the increased formation of "inactive" and undesirable spectator species would correlate favorably with the observed activities.

As we recently reported,[20] UV−vis analysis confirms that 0.5Fe-silicalite-1_{900} has "over-clustered" to Fe oxide species upon the excessive thermal pretreatment (Supplementary Table S1). Indeed, a remarkable increase in the fraction of undesirable larger clusters and bulk oxides is observed following pretreatment at 900 °C. This agrees well with the color of the sample (orange/brown) and the significant decrease in observed activity (Figure 2). It is apparent, therefore, that once a given amount of Fe migrates from the framework of 0.5Fe-silicalite-1, the formation of larger clusters and bulk Fe oxides is triggered, and the catalyst rapidly decreases in activity.

In contrast, despite Fe^{3+} apparently being more readily extracted from the MFI framework in 0.5Fe-ZSM-5 (84) than 0.5Fe-silicalite-1 to begin with, the pretreated samples of 0.5Fe-ZSM-5 $(90)_{750}$ and 0.5Fe-ZSM-5 $(84)_{900}$ do not possess significantly different Fe speciation to the sample calcined at 550 °C, and the fraction of "active" extra-framework Fe^{3+} species within the zeolite micropores does change significantly. This correlates favorably with the miminal decrease in activity observed with these samples. Although the pretreatment of 0.5Fe-ZSM-5 (84) at high temperatures (>550 °C) will also

dx.doi.org/10.1021/cs400288b | *ACS Catal.* 2013, 3, 1835−1844

lead to some dealumination, i.e., the formation of extra-framework Al^{3+}, the fraction of such octahedral Al^{3+} remained low, in agreement with the known stability of framework Al^{3+} in MFI frameworks. Furthermore, the pretreatment of ZSM-5 (86) at such temperatures still did not lead to any relevant catalytic activity, thus demonstrating that the changes in Fe^{3+} speciation are the dominant factor in the activity of these materials.

The observation that the "over-clustering" of Fe^{3+} to larger clusters and bulk Fe oxides is less prevalent for 0.5Fe-ZSM-5 (84) than for 0.5Fe-silicalite-1 suggests that an alternative promotional role of Al^{3+} may be its ability to stabilize or disperse the active extra-framework cationic Fe species, as previously observed by groups focusing on gas-phase oxidation of higher hydrocarbons and NO_x decomposition.[21,29−31] Should this be the case, it would be expected that this would particularly apply for active catalytic materials prepared by postdeposition methods; although we have shown these samples to be less active per mole of Fe^{3+}, they contain the entire Fe^{3+} fraction in extra-framework positions and thus allow the discrimination of Al^{3+} promotion through dispersion/stabilization and the increased extraction phenomena observed for the hydrothermally prepared samples. Thus, samples of 2.5 wt % Fe^{3+}/ZSM-5 (86) and 2.5 wt % Fe^{3+}/silicalite-1 were prepared by solid-state ion exchange and screened for catalytic activity. The higher metal loading (2.5 wt % vs 0.5 wt %) was chosen given the lower intrinsic activity of postsynthetic deposition compared to hydrothermal incorporation. We note here that postsynthetic Fe^{3+} deposition is denoted Fe^{3+}/ZSM-5, whereas hydrothermal incorporation is defined Fe-ZSM-5.

Figure 4 demonstrates that despite identical Fe^{3+} loadings (2.5 wt %) and pretreatment conditions (550 °C, 3 h, static air), the 2.5Fe^{3+}/ZSM-5 $(86)_{550}$ sample is more than 1 order of magnitude more active than the analogous 2.5Fe^{3+}/silicalite-1_{550}. This clearly emphasizes that there is a beneficial role of Al^{3+} that is not related to its ability to facilitate the extraction of Fe^{3+} from the framework of the zeolite, as both samples were prepared by postdeposition methods and did not therefore contain any (initial) framework Fe^{3+}.

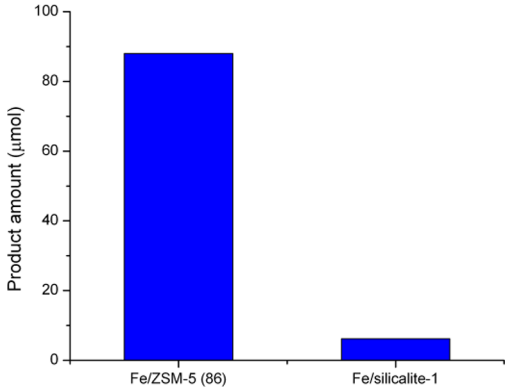

Figure 4. Catalytic activity of 2.5 wt % Fe/ZSM-5 (86) and 2.5 wt % Fe/silicalite-1, prepared by solid-state ion exchange. Reaction conditions: cat., various (27 mg); $P_{(CH_4)}$, 30.5 bar; [H_2O_2], 0.5 M; temp, 50 °C; time, 30 min; stirring speed, 1500 rpm. Note: catalyst pretreatment, 550 °C, 3 h, static air.

Following deconvolution of the relevant UV−vis spectra of 2.5Fe^{3+}/silicalite-1_{550} and 2.5Fe^{3+}/ZSM-5 $(86)_{550}$, it is clear that 2.5Fe^{3+}/silicalite-1_{550} possesses a significantly lower fraction of "active" Fe species than 2.5Fe^{3+}/ZSM-5 $(86)_{550}$ (Table 4). While we could expect 2.5Fe^{3+}/silicalite-1 to thus be around one-third the activity of 2.5Fe^{3+}/ZSM-5, based on the relative contributions within each sample, it cannot be overlooked that the UV−vis spectrum of 2.5Fe^{3+}/silicalite-1 is dominanted by larger Fe clusters and bulk Fe oxides, which are responsible for nonselective H_2O_2 decomposition (entry 2).[20] On the other hand, the fraction of such undesirable spectator species in 2.5Fe^{3+}/ZSM-5 (86) is much lower. The lack of active sites, coupled with the large amount of undesirable Fe species, results in this sample showing little activity whatsoever. It is clear therefore that Fe^{3+} is significantly more dispersed within/on the MFI material when Al^{3+} is also present in the zeolite structure, as significantly less bulk oxides (and thus less clustering) is observed in 2.5Fe^{3+}/ZSM-5 $(86)_{550}$ than in 2.5Fe^{3+}/silicalite-1_{550}.

Table 4. Deconvolution Data for 2.5Fe^{3+}/Silicalite-1_{550} and 2.5Fe^{3+}/ZSM-5 $(86)_{550}$[a]

	relative contribution of each λ range (nm)			
catalyst	λ_1	λ_2	λ_3	λ_4
2.5Fe^{3+}/silicalite-1_{550}	0.204	0.164	0.236	0.395
2.5Fe^{3+}/ZSM-5 $(86)_{550}$	0.169	0.512	0.192	0.127

[a]Data calculated from UV−vis spectra in Supplementary Figure S4.

On the basis of these experiments, it is evident that the inclusion of Al^{3+} within the zeolite leads to higher levels of activity, due to both an increased extraction of Fe^{3+} from the zeolite framework (where applicable) *and* an increased dispersion of the extra-framework Fe species, which maximizes the fraction of extra-framework Fe species within the zeolite micropores and minimizes the fraction of undesirable clusters and bulk oxides. Nevertheless, the exact nature of this increased dispersion is not yet evident. Previously, it has been proposed that Al^{3+} aids the dispersion of Fe^{3+} in similar zeolite materials even when deposited by postsynthesis methods; from this, it has been proposed that extra-framework Al^{3+} species are able to aid dispersion.[21] Alternatively, the cation-exchange sites associated with framework Al^{3+} may also be responsible for dispersion, given the ability of the negative lattice charge to coordinate and stabilize cationic complexes.[24,25] Nevertheless, each of these studies utilized Fe-containing zeolites for high-temperature (>250 °C) gas-phase oxidation chemistry, which we have shown to be unrelated to our present system. Furthermore, both reported catalytic systems required pretreatment at significantly higher temperatures compared to the catalysts reported herein and in a vacuum or an inert atmosphere, in order to facilitate the formation of Fe^{2+} species that are responsible for activity in such cases. Thus, the extrapolation of these previous studies to the present system, which focuses on the low-temperature, aqueous-phase methane oxidation with Fe^{3+} active sites cannot be presumed.

To probe whether framework or extra-framework Al^{3+} species were responsible for the promotion, Al^{3+} was incorporated into 0.5Fe-silicalite-1 by three different techniques, namely, hydrothermal synthesis, solid-state ion exchange, and impregnation. From the data presented (Figure 5), it is clear that the addition of Al^{3+} to 0.5Fe-silicalite-1_{550} by solid-state ion exchange or impregnation does not lead to any improvements in catalytic activity. It can thus be firmly concluded that extra-framework Al^{3+} species do not promote the catalytic activity of Fe^{3+} and that an extra-framework mixed

dx.doi.org/10.1021/cs400288b | ACS Catal. 2013, 3, 1835−1844

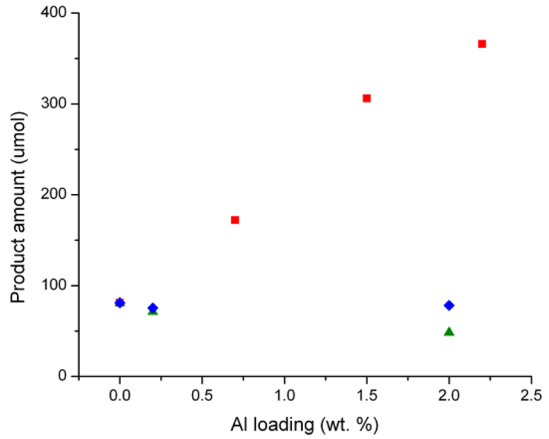

Figure 5. Influence of Al^{3+} addition on the catalytic activity of 0.5Fe-silicalite-1_{550}. For the postsynthesis samples, Al^{3+} was added to a presynthesized sample of 0.5Fe-silicalite-1. For 0.5Fe-ZSM-5 (X) prepared by hydrothermal synthesis, Fe *and* Al were concurrently incorporated into the framework by the addition of the relevant precursors to the synthesis gel. (■) Hydrothermal incorporation, (▲) impregnation, (♦) solid-state ion exchange. Reaction conditions: volume, 10 mL; time, 30 min; temp, 50 °C; $P_{(CH_4)}$, 30.5 bar; $[H_2O_2]$, 0.5 M; catalyst, 27 mg; stirring speed, 1500 rpm; catalyst pretreatment, calcination (550 °C, 3 h, static air).

oxide (Fe-O-Al) is highly unlikely to be responsible for catalytic activity, as has previously been proposed for N_2O-based oxidations.[21]

In contrast, the incorporation of Al^{3+} into the framework of 0.5Fe-silicalite-1_{550} during hydrothermal synthesis leads to significant increases in catalytic activity, which are directly proportional to the Al^{3+} content up to 2.2 wt %. Given that this method is the only method capable of incorporating Al^{3+} into the zeolite framework and is thus the only method capable of increasing the number of cation-exchange sites, it can be proposed that the increased cation-exchange site density is responsible for the promotion displayed by Al^{3+}, presumably by the stabilization and dispersion of the active Fe^{3+} cations onto the negative framework charge associated with the AlO_4^- tetrahedron. This would lead to a more significant interaction between extra-framework Fe^{3+} and the zeolite framework (anchoring) and would limit the formation of bulk and undesirable oxide species upon pretreatment. We note here that while the observed TOF for the most active sample (0.5Fe-ZSM-5 $(28)_{550}$) is still around 5−10 times lower than the highest obtained with commercial 0.014ZSM-5 $(30)_{550}$ under identical reaction conditions,[18] we reason that the probability of obtaining the highest percentage of active Fe sites while concurrently minimizing the formation of undesirable Fe oxides is likely to be increased at lower Fe loadings. This will be described in depth in the following section.

To substantiate the proposed interaction of cationic extra-framework Fe^{3+} and framework Al^{3+}, 2.5Fe^{3+}/ZSM-5 $(86)_{550}$ was investigated with FT-IR spectroscopy. It is well-known that when in the H^+-form, the cation-exchange sites associated with framework T^{3+} atoms give rise to clear stretches between 3700 and 3600 cm^{-1}, the exact values of which depend entirely on the identity of the T^{3+} atom. If cationic Fe complexes are indeed dispersed on the cation-exchange sites, the intensity of the Al-O(H)-Si stretch (3610 cm^{-1}) should diminish taking into account that some (or all) of the protons would be replaced by cationic Fe complexes. This was subsequently verified experimentally, as the Al-O(H)-Si band in ZSM-5 (86) (Figure 6, A/blue) is completely eliminated from the FT-IR

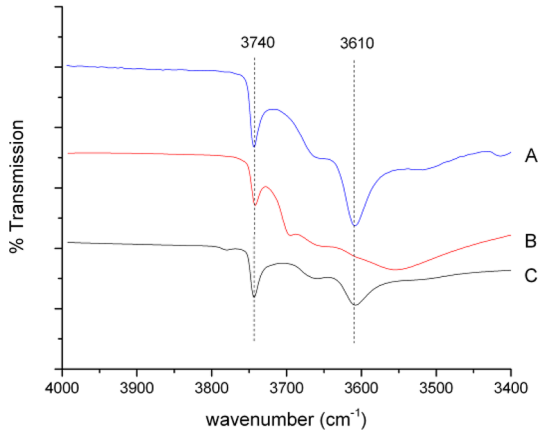

Figure 6. O−H stretching region of the FT-IR spectra of ZSM-5 (86) (A/blue), uncalcined/as synthesized 2.5 wt % Fe^{3+}/ZSM-5 (86) (B/red) and calcined 2.5 wt % Fe^{3+}/ZSM-5 (86) (C/green). Absorbances were normalized to the Si−O−Si stretches of the zeolite framework.

spectrum upon solid-state ion exchange with Fe^{3+} (B/red). This indicates the substitution of all of the cation-exchange sites with Fe^{3+} during catalyst synthesis and confirms the association of extra-framework Fe^{3+} with the cation-exchange sites associated with framework Al^{3+}. Nevertheless, despite the excess of Fe to Al in these samples, a partial restoration of the Al-O(H)-Si band is observed after calcination the final catalyst at 550 °C. The lack of 100% exchange, i.e., complete loss of the O−H band, in this sample, which is the active catalyst, is likely due to increased clustering of Fe^{3+} into larger clusters or bulky iron oxides upon calcination.

To further substantiate the hypothesis that framework Al^{3+} maximizes the formation of the active Fe^{3+} species, a final analogous sample of [Fe,Ga]-silicalite-1 was prepared by hydrothermal synthesis. This substitution of Si^{4+} by Ga^{3+} also gives rise to cation-exchange sites in a similar manner to Al^{3+} and a significant increase in catalytic activity versus the Fe-only analogue (Figure 7). This strengthens the identification of

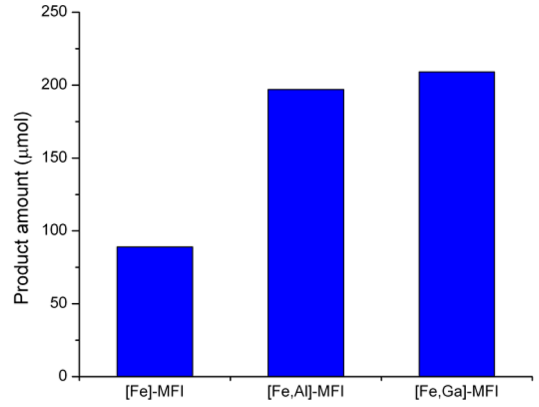

Figure 7. Catalytic activity of various Fe-containing zeolites at a fixed Fe loading (0.5 wt %). Ga^{3+} and Al^{3+}, where applicable, were added to the material at an SiO_2/M_2O_3 ratio of ±85. Reaction conditions: cat., various (27 mg); $P_{(CH_4)}$, 30.5 bar; $[H_2O_2]$, 0.5 M; temp, 50 °C; time, 30 min; stirring speed, 1500 rpm. Note: catalyst pretreatment, 550 °C, 3 h, static air.

dx.doi.org/10.1021/cs400288b | *ACS Catal.* 2013, 3, 1835−1844

cation-exchange sites as the promoting functionality of the zeolite in this process. Moreover, other similarities to the [Fe,Al] system were observed in that the incorporation of Ga^{3+} alone into the MFI material was insufficient for catalytic activity and that postsynthesis deposition of Ga^{3+} was also not beneficial to the activity of the catalyst (Supplementary Table S2). It is again clear that significant promotion is observed *only* when a trivalent heteroatom is incorporated into the zeolite framework, thus leading to increased cation-exchange site density.

Optimized Material Synthesis. At this point, we have established (1) that the catalytic activity of (Fe)-ZSM-5 correlates to the presence of extra-framework Fe^{3+} species within the zeolitic micropores (work herein and ref 20), (2) that the clustering of extra-framework Fe^{3+} to larger clusters and bulk oxides leads to a decrease in activity and C- and H_2-based selectivity,[20] and (3) that the copresence of Al^{3+} or Ga^{3+} is critical for maximizing the activity of each Fe^{3+} atom, first by facilitating its extraction from the zeolitic framework, and second by providing cation-exchange sites that are capable of acting as stabilizing ligands to the cationic Fe^{3+} species, thereby inhibiting the formation of undesirable side species and maximizing the fraction of active species. Nevertheless, the TOFs exhibited by the optimal material so far, 0.5Fe-ZSM-5 $(28)_{550}$, are still around 5−10 times lower than those exhibited by commercial ZSM-5 (30), containing only 0.014 wt % Fe.[18]

By considering these factors, we reasoned that the extremely high TOFs of the commercial sample might be due primarily to its low Fe loading (0.014 wt %) but high Al loading (2.3 wt %); a large amount of Al^{3+} would maximize the extraction of framework Fe^{3+} (thereby forming a greater number of active sites) and provide sufficient cation-exchange sites to stabilize *all* of the extracted Fe^{3+} (thereby inhibiting the formation of undesirable side species). The low Fe loading would also maximize the percentage of "active" Fe species, as the spatial distribution of Fe would be maximized and the formation of bulk oxides inhibited. In view of this, a number of Fe- and Al-containing ZSM-5 samples were prepared (Figure 8).

Many important features are immediately evident from the data shown in Figure 8. First, it is clear that as the Al content of the material increases, the activity of each catalyst at a given Fe loading is higher, likely due to the more facile extraction of framework Fe^{3+} at higher Al contents. Furthermore, it is clear that at higher Al contents the optimal Fe loading decreases. It is likely that due to the increased extraction, the possibility of forming inactive larger clusters and bulk oxides is enhanced at higher loadings. Finally, it is apparent that above the optimal Fe loading of each Fe-ZSM-5 (X) series, catalytic activity decreases, yet the apparent decrease in activity is much lower at higher Al^{3+} content. This is in excellent agreement to our previous observations and confirms that Al^{3+} inhibits the formation of larger Fe clusters and Fe oxides, thus maximizing the amount of active Fe species and minimizing the amount of undesirable side species. Each of these observations fully supports the hypothesis that the key to attaining the highest levels of activity is maximizing the content of Al^{3+} and subsequently optimizing the Fe content.

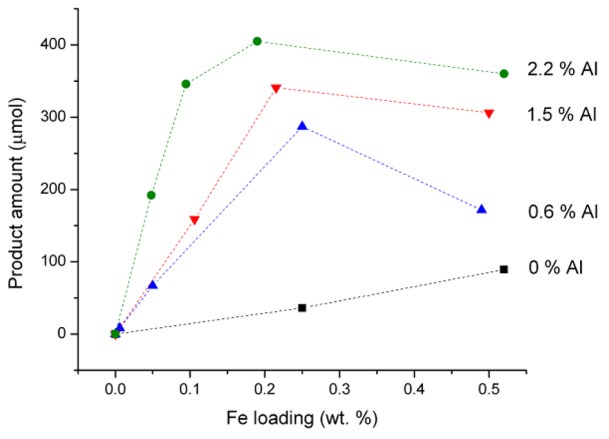

Figure 8. Catalytic activity of various Fe-ZSM-5 samples containing different Fe and Al contents. Reaction conditions: cat., various (27 mg); $P_{(CH_4)}$, 30.5 bar; $[H_2O_2]$, 0.5 M; temp, 50 °C; time, 30 min; stirring speed, 1500 rpm. Note: catalyst pretreatment, 550 °C, 3 h, static air.

We note here that we have previously proposed through EXAFS analysis and DFT calculations that catalytic activity is due to an extra-framework species, $[Fe_2(\mu_2\text{-}OH)_2(OH)_2(H_2O)_2]^{2+}$, a binuclear active site that comprises an overall +2 charge.[18] The coordination of such a species on to the cation-exchange sites would require two exchange sites within a critical distance of ∼5−6 Å, or two Al^{3+} atoms within the 10 membered MFI ring. The probability of having two exchange sites within this distance would improve significantly upon the incorporation of additional Al^{3+} into the framework and has been shown by Feng and Hall to be very high for zeolites with a SiO_2/Al_2O_3 mole ratio approaching 40, but negligible for zeolites with a SiO_2/Al_2O_3 much greater than 100.[33] This correlates favorably with the observed activity.

It is important to stress here that by understanding the critical role(s) of each component of the catalyst, we have been able to optimize the catalytic activity of Fe-ZSM-5 enormously. The TOFs displayed by the Fe-ZSM-5 (28) series, containing 2.2 wt % Al, are 2 orders of magnitude higher than those of the Fe-only series, i.e., 0.5Fe-silicalite-1. Thus, the TOFs exhibited by this series are now very similar to the TOFs obtained for the original commercial ZSM-5 (30) catalyst, the most intrinsically active catalyst to date. For example, 0.045Fe-ZSM-5 $(28)_{550}$ and 0.095Fe-ZSM-5 $(28)_{550}$ oxidize methane at a TOF of ca. 1,600 h^{-1}, comparable to the ca. 2,000 h^{-1} that we have observed for commercial ZSM-5 $(30)_{550}$. More importantly, however, is that these levels of TOF have been maintained at significantly higher Fe loadings (0.095 wt % vs 0.014 wt %). Thus, along with possessing similar intrinsic activity, 0.095Fe-ZSM-5 (28) is around 5 times more productive in terms of volumetric productivity (1.92×10^{-8} mol (product) cm^{-3} s^{-1} after 30 min) than commercial ZSM-5 (30) (4.2×10^{-9} mol cm^{-3} s^{-1} after 30 min).

CONCLUSIONS

Through catalytic measurements and spectroscopic investigations, we have demonstrated that while extra-framework Fe^{3+} species are the active component of Fe-containing MFI-type zeolites for selective aqueous-phase methane oxidation, significant promotion is observed upon the incorporation of other noncatalytic trivalent cations (e.g., Al^{3+} or Ga^{3+}) into the MFI-framework. We have rationalized this promotion in terms of two co-operative effects. First, the coaddition of Al^{3+} or Ga^{3+} to the framework leads to an increased migration of (initially) framework Fe^{3+} to the extra-framework during heat pretreatment. Concurrently, the cation-exchange sites associated with framework M^{3+} species also are able to stabilize and disperse

dx.doi.org/10.1021/cs400288b | ACS Catal. 2013, 3, 1835−1844

the so-formed extra-framework Fe^{3+} species that are responsible for catalytic activity. In this case, the dispersion of Fe^{3+} is a consequence of both the dispersed nature of Al^{3+} within the zeolite (Lowenstein's rules ensuring maximum dispersion) and an "anchoring" process whereby Fe is inhibited toward agglomeration into bulk oxides due to the stabilization provided by the negative framework charge. By understanding these key roles exhibited by each aspect of the solid catalyst, significant improvements in catalytic activity (2 orders of magnitude) have been obtained by the careful and rationalized design of new catalysts. Optimal activity has thus been obtained with a catalyst comprising 0.095 wt % Fe and 2.2 wt % of Al^{3+}. This catalyst performs this highly desirable reaction at volumetric productivities of 1.92×10^{-8} mol cm^{-3} s^{-1} (averaged over 30 min) and at TOFs comparable to that of the commercial catalyst previously reported (ca. 2,000 h^{-1} averaged over 30 min) and is therefore the most active catalyst reported for this challenging reaction to date.

EXPERIMENTAL SECTION

Catalyst Synthesis and Pretreatment. MFI-type zeolites containing various amounts of Fe, Al, and Ga were prepared by a hydrothermal synthesis method in a batch autoclave. The procedure used is more completely described previously.[18,20] Crystallization was performed in a stainless-steel autoclave at 175 °C for 120 h. The as-synthesized materials obtained were calcined at 550 °C (1 °C min^{-1}), first in a flow of nitrogen (5 h) and later air (3 h) in order to remove the organic template. The detemplated sample was subsequently ion-exchanged three times with NH_4NO_3 (1.0 M) at 95 °C and later dried for 16 h at 110 °C. Activation was achieved by calcination in flowing air (30 mL min^{-1}) at 550, 750, or 900 °C for 3 h. Following this route, ferrigallosilicate ([Fe, Ga]), ferrisilicate ([Fe]), aluminosilicate ([Al]), and silicate (no heteroatom) were also prepared.

Silicalite-1, Fe-silicalite-1, and ZSM-5 were also used as precursors for the incorporation of Al^{3+}, Fe^{3+}, and Ga^{3+} by postsynthesis deposition methods (impregnation, solid state, and aqueous ion exchange). To this end, 2.5 wt %Fe/ZSM-5 was prepared by impregnation through the addition of support (1.95 g, NH_4-ZSM-5, SiO_2/Al_2O_3 molar ratio = 30, Zeolyst) to an aqueous solution of $Fe(NO_3)_3 \cdot 9H_2O$ (3.613 mL, 13.828 g dissolved in 1 L). The solution was stirred until a homogeneous solution was obtained. The slurry was dried (16 h, 110 °C) before calcination at 550 °C for 3 h in static air. Also, 2.5 wt % Fe/ZSM-5 was prepared by solid-state ion exchange by adding the desired amount of $Fe(acac)_3$ (0.158 g, 0.45 mmol) to NH_4-ZSM-5 (0.975 g, SiO_2/Al_2O_3 molar ratio = 30, Zeolyst) prior to mechanical grinding for 30 min. Finally, aqueous ion exchange of was performed by the addition of NH_4-ZSM-5 (2 g, SiO_2/Al_2O_3 molar ratio = 30, Zeolyst) to an aqueous solution of $Fe(NO_3)_3 \cdot 9H_2O$ (30 mL, 0.02 M, 20.2 g $Fe(NO_3)_3 \cdot 9H_2O$ dissolved in 250 mL of deionized water). The suspension was stirred vigorously (85 °C, 24 h) under reflux. The catalyst was filtered, washed with deionized water, and dried (16 h, 110 °C). Prior to testing, the catalyst was activated by calcination at 550 °C for 3 h in static air.

Catalyst Characterization. Powder X-ray diffraction (XRPD) was performed using a PANalytical X'PertPRO X-ray diffractometer, with a Cu Kα radiation source (40 kV and 40 mA). Diffraction patterns were recorded between 6° and 55° 2θ at a step size of 0.0167° (time/step = 150 s, total time = 1 h). FT-IR spectroscopy was performed by forming self-supporting wafers from a small amount of sample and KBr. The spectra were recorded on a Jasco FT-IR660 Plus over a range of 4000−400 cm^{-1} at a resolution of 2 cm^{-1}. UV−vis analysis was performed on an Agilent Cary 4000 UV−vis spectrophotometer equipped with diffuse reflectance setup. Samples were scanned between 190 and 900 nm at a scan rate of 600 nm min^{-1}. Na, Si, and Al content was determined by Neutron Activation Analysis (NAA). Metal contents were determined by ICP-OES to an accuracy of ±10

Kinetic Evaluation. Microkinetic analysis was carried out in a batch stainless steel autoclave (Parr Autoclaves) containing a Teflon liner vessel and a working volume of 35 mL. The vessel was charged with an aqueous solution of H_2O_2 (10 mL, 0.5 M, 5000 μmol) and the desired amount of catalyst (typically 27 mg). After evacuation of contaminant gases, the autoclave was heated to the reaction temperature (typically 50 °C) and vigorously stirred at 1500 rpm once the desired temperature was obtained. The vessel was cooled in ice (12 °C) following the appropriate reaction time, and the resultant solution was filtered and analyzed. Experimental error was determined to be ±7%.

Analytical Methods. Aqueous-phase products were identified through ^1H NMR spectroscopy on a Bruker 500 MHz Ultra-Shield NMR spectrometer and quantified against a 1 vol % TMS/$CDCl_3$ internal standard, previously calibrated against authentic standards. The detection limit was optimized to a level corresponding to a product yield of 0.1 μmol.[20] End H_2O_2 concentrations were determined by titration against acidified $Ce(SO_4)_2$ solution. Gas-phase products were quantified by means of an FID-GC (Varian 450-GC) fitted with a CP-Sil 5CB capillary column (50 m length, 0.32 mm i.d.). The GC was equipped with a methaniser unit, and CO_2 was quantified against a calibration curve constructed from commercial standards (BOC).

ASSOCIATED CONTENT

Supporting Information

This material is available free of charge via the Internet at http://pubs.acs.org.

AUTHOR INFORMATION

Corresponding Author

*E-mail: ceri.hammond@chem.ethz.ch; hutch@cardiff.ac.uk.

Present Addresses

[‖]Department of Chemistry and Applied Biosciences, ETH Zürich, Wolfgang-Pauli-Str. 10, CH-8093 Zürich, Switzerland.
[⊥]University College London, 20 Gordon Street, WC1H 0AJ London, U.K. and Research Complex at Harwell, Rutherford Appleton Laboratory, Harwell Oxford, Didcot OX11 0FA, U.K.
[#]Stephenson Institute for Renewable Energy, Chemistry Department, The University of Liverpool, Crown Street, Liverpool L69 7ZD, U.K.

Notes

The authors declare no competing financial interest.

ACKNOWLEDGMENTS

This work formed part of the Methane Challenge. The Dow Chemical Company is thanked for their financial support. Computing facilities for this work were provided by ARCCA at Cardiff University, HPC Wales, and the UK's HPC Materials Chemistry Consortium (MCC). The MCC is funded by EPSRC (EP/F067496).

ABBREVIATIONS AND DEFINITIONS

Partial oxygenated products: methyl hydroperoxide (CH_3OOH), methanol (CH_3OH), and formic acid (HCOOH); total product formed: partial oxygenates + CO_2; oxygenate selectivity: [moles (partial oxygenates)]/[mols (total oxygenated product)] × 100; turnover frequency: moles (oxygenated species formed) mol^{-1} (Fe) h^{-1}; volumetric productivity: moles (oxygenated species formed) cm^{-3} (reactor volume) s^{-1}. Volumetric productivity and TOFs were calculated on the basis of the final yield at the end of the reaction, i.e., they are an averaged value over the entire time scale of the reaction. Typically, the initial productivities and

TOFs, i.e., productivities at 2 and 5 min of reaction, were 1−2 orders of magnitude higher.

REFERENCES

(1) Hammond, C.; Conrad, S.; Hermans, I. *ChemSusChem* **2012**, *5*, 1668.
(2) Golisz, S. R.; Gunnoe, T. B.; Goddard, W. A., III; Groves, J. T.; Periana, R. A. *Catal. Lett.* **2011**, *141*, 213.
(3) Hammer, G.; Lubcke, T.; Kettner, R.; Pillarella, M. R.; Recknagel, H.; Commichau, A.; Neumann, H.-J.; Paczynska-Lahme, B. In *Ullmann's Encyclopaedia of Industrial Chemistry*; Wiley-VCH: Weinheim, 2006; Vol. *23*, p 739.
(4) Fiedler, E.; Grossmann, G.; Keresbohm, D. B.; Weiss, G.; Witte, C. In *Ullmann's Encyclopaedia of Industrial Chemistry*; Wiley-VCH: Weinheim, 2011; Vol. *23*, p 26.
(5) Chang, C. D.; Silvestri, A. J. *J. Catal.* **1977**, *47*, 249.
(6) Periana, R. A.; Taube, D. J.; Gamble, S.; Taube, H.; Satoh, T.; Fujii, H. *Science* **1998**, *280*, 560.
(7) Palkovits, R.; Antonietti, M.; Kuhn, P.; Thomas, A.; Schueth, F. *Angew. Chem., Int. Ed.* **2009**, *48*, 6909.
(8) Dubkov, K. A.; Sobolev, V. I.; Panov, G. I. *Kinet. Catal.* **1998**, *39*, 72.
(9) Dubkov, K. A.; Sobolev, V. I.; Talsi, E. P.; Rodkin, M. A.; Watkins, N. H.; Shteinman, A. A.; Panov, G. I. *J. Mol. Catal A: Chem.* **1997**, *123*, 155.
(10) Groothaert, M. H.; Smeets, P. J.; Sels, B. F.; Jacobs, P. A.; Schoonheydt, R. A. *J. Am. Chem. Soc.* **2005**, *127*, 1394.
(11) Vanelderen, P.; Hadt, R. G.; Smeets, P. J.; Solomon, E. I.; Schoonheydt, R. A.; Sels, B. F. *J. Catal.* **2011**, *284*, 157.
(12) Himes, R. A.; Karlin, K. D. *Curr. Opin. Chem. Biol.* **2009**, *13*, 119.
(13) Himes, R. A.; Karlin, K. D. *Proc. Natl. Acad. Sci. U.S.A.* **2009**, *106*, 18877.
(14) Raja, R.; Ratnasamy, P. *Appl. Catal., A* **1997**, *158*, L7.
(15) Sorokin, A. B.; Kudrik, E. V.; Alvarez, L. X.; Afanasiev, P.; Millet, J. M. M.; Bouchu, D. *Catal. Today* **2010**, *157*, 149.
(16) Sorokin, A. B.; Kudrik, E. V.; Bouchu, D. *Chem. Commun.* **2008**, 2562.
(17) Forde, M. M.; Grazia, B. C.; Armstrong, R.; Jenkins, R. L.; Ab Rahim, M. H.; Carley, A. F.; Dimitratos, N.; Lopez-Sanchez, J. A.; Taylor, S. H.; McKeown, N. B.; Hutchings, G. J. *J. Catal.* **2012**, *290*, 177.
(18) Hammond, C.; Forde, M. M.; Ab Rahim, M. H.; Thetford, A.; He, Q.; Jenkins, R. L.; Dimitratos, N.; Lopez-Sanchez, J. A.; Dummer, N. F.; Murphy, D. M.; Carley, A. F.; Taylor, S. H.; Willock, D. J.; Stangland, E. E.; Kang, J.; Hagen, H.; Kiely, C. J.; Hutchings, G. J. *Angew. Chem., Int. Ed.* **2012**, *51*, 5129.
(19) Hammond, C.; Jenkins, R. L.; Dimitratos, N.; Lopez-Sanchez, J. A.; ab Rahim, M. H.; Forde, M. M.; Thetford, A.; Murphy, D. M.; Hagen, H.; Stangland, E. E.; Moulijn, J. M.; Taylor, S. H.; Willock, D. J.; Hutchings, G. J. *Chem.—Eur. J.* **2012**, *18*, 15735.
(20) Hammond, C.; Dimitratos, N.; Jenkins, R. L.; Lopez-Sanchez, J. A.; Kondrat, S. A.; Ab Rahim, M. H.; Forde, M. M.; Thetford, A.; Taylor, S. H.; Hagen, H.; Stangland, E. E.; Kang, J.; Moulijn, J. M.; Willock, D. J.; Hutchings, G. J. *ACS Catal.* **2013**, *3*, 689−699.
(21) Hensen, E. J. M.; Zhu, Q.; Janssen, R. A. J.; Magusin, P.; Kooyman, P. J.; van Santen, R. A. *J. Catal.* **2005**, *233*, 123.
(22) Notte, P. P. *Top. Catal.* **2000**, *13*, 387.
(23) Hensen, E. J. M.; Zhu, Q. J.; Liu, P. H.; Chao, K. J.; van Santen, R. A. *J. Catal.* **2004**, *221*, 560.
(24) Battiston, A. A.; Bitter, J. H.; Heijboer, W. M.; de Groot, F. M. F.; Koningsberger, D. C. *J. Catal.* **2003**, *215*, 279.
(25) Battiston, A. A.; Bitter, Koningsberger, D. C. *J. Catal.* **2003**, *218*, 163.
(26) Zecchina, A.; Rivallan, M.; Berlier, G.; Lamberti, C.; Ricchiardi, G. *Phys. Chem. Chem. Phys.* **2007**, *9*, 3483.
(27) Bordiga, S.; Buzzoni, R.; Geobaldo, F.; Lamberti, C.; Giamello, E.; Zecchina, A.; Leofanti, G.; Petrini, G.; Tozzola, G.; Vlaic, G. *J. Catal.* **1996**, *158*, 486.
(28) Perez-Ramirez, J.; Groen, G. C.; Bruckner, A.; Kumar, M. S.; Bentrup, U.; Debbagh, M. N.; Villaescusa, L. A. *J. Catal.* **2005**, *232*, 318−334.
(29) Kumar, A. S.; Perez-Ramirez, J.; Debbagh, M. N.; Smarsly, B.; Bentrup, U.; Bruckner, A. *Appl. Catal., B* **2006**, *62*, 244.
(30) Perez-Ramirez, J.; Groen, J. C.; Bruckner, A.; Kumar, M. S.; Bentrup, U.; Debbagh, M. N.; Villaescusa, L. A. *J. Catal.* **2005**, *232*, 318.
(31) Hensen, E. J. M.; Zhu, Q.; Hendrix, M.; Overweg, A. R.; Kooyman, P. J.; Sychev, M. V.; van Santen, R. A. *J. Catal.* **2004**, *221*, 560.
(32) Perez-Ramirez, J. *J. Catal.* **2004**, *227*, 512.
(33) Feng, X. B.; Hall, W. K. *J. Catal.* **1997**, *166*, 368.